

Reflection high-energy electron diffraction study of the molecular beam epitaxial growth of CaF_2 on $\text{Si}(110)$

W. K. Liu

*Department of Physics and Astronomy and Laboratory for Electronic Properties of Materials,
University of Oklahoma, Norman, Oklahoma 73019*

X. M. Fang and P. J. McCann

*School of Electrical Engineering and Laboratory for Electronic Properties of Materials,
University of Oklahoma, Norman, Oklahoma 73019*

(Received 25 April 1995; accepted for publication 18 July 1995)

Molecular beam epitaxial growth of CaF_2 on $\text{Si}(110)$ was studied using reflection high-energy electron diffraction (RHEED) and scanning electron microscopy (SEM). An optimum substrate temperature range exists between 800 and 900 °C within which (110)-oriented epitaxy can be sustained. At the initial growth stage, long strips of CaF_2 parallel to the $[\bar{1}10]$ direction are formed due to the growth anisotropy on the (110) surface. This is followed by the development of low-energy $\{111\}$ facets, producing a ridged and grooved surface morphology. Growth then proceeds via the stacking of $\{111\}$ planes on the sidewalls of the ridges. This surface morphology is believed to result from the combination of favorable energetics in exposing the low-energy $\{111\}$ facets and the presence of twinned crystallographic domains. © 1995 American Institute of Physics.

Epitaxial layers of group II fluoride insulators grown on Si and other substrates have been studied for a variety of potential applications such as in semiconductor-on-insulator structures, metal-insulator-semiconductor devices, surface passivation, electron beam resist, and buffer layers for heteroepitaxy.¹ Recently, interest has shifted towards using epitaxial fluorides as rare-earth dopant hosts for solid state microlaser fabrication.²⁻⁶ For example, neodymium (Nd)⁵ and erbium (Er)⁶ doped CaF_2 layers grown on Si substrates have exhibited strong photoluminescence at 1.04 and 1.54 μm , respectively. With suitable optical feedback cavities, it is possible to fabricate lasers on Si substrates using these materials. A potentially attractive substrate for in-plan laser fabrication is $\text{Si}(110)$. Parallel cleavage faces, and hence Fabry-Perot cavities, can be obtained by cleaving the CaF_2 layer along two of the four $\{111\}$ cleavage planes that intersect the (110) surface at 90°. Earlier work by Schowalter *et al.*^{1,7} showed that CaF_2 grows on $\text{Si}(110)$ via ridges and grooves running along the $\langle 110 \rangle$ directions. In this letter, we confirm this earlier result^{1,7} as well as present detailed *in situ* reflection high-energy electron diffraction (RHEED) and scanning electron microscopy (SEM) data on the molecular beam epitaxial (MBE) growth of CaF_2 on $\text{Si}(110)$. We also propose a growth model to explain the observed ridged and grooved surface morphology. Our results, which concern initial growth kinetics and the effect of growth parameters on the surface morphology, should prove useful for subsequent fabrication of solid state microlasers on $\text{Si}(110)$ substrates.

CaF_2 growth was carried out in an Intevac modular GEN-II MBE system equipped with a Varian electron gun operated at 9.5 keV for *in situ* RHEED observations. A high purity polycrystalline CaF_2 source was evaporated from a graphite-coated PBN crucible. Background pressure in the range of 10^{-10} Torr was maintained throughout deposition.

Beam equivalent pressure (BEP) of $\sim 7.0 \times 10^{-8}$ Torr was used, resulting in a growth rate of approximately 20 Å/min. Substrate temperatures (T_{sub}) were measured, by a thermocouple located at the center of the substrate heater and were varied from 700 to 900 °C in this study. All samples were grown on 3 in. diam *p*-type $\text{Si}(110)$ substrates (Silicon Sensen, Inc.) cleaned using the Shiraki method.⁸ The passivating oxide formed during the *ex situ* cleaning procedure was thermally desorbed in the growth chamber at ~ 1100 °C as confirmed by Auger electron spectroscopy.

We have previously shown that RHEED characterization, in spite of the known effects of electron-beam-induced fluorine desorption, can be used to analyze the growth mode during fluoride deposition.⁹ Electron beam irradiation time was kept to a minimum and RHEED patterns recorded at different growth stages were taken from previously unexposed areas to ensure that the observed diffraction features reflected real growth morphology and were not related to electron-beam induced artifacts. Digitized images of these patterns were obtained using a CCD camera and a data acquisition system developed by *k*-Space Associates, Inc. Scanning electron microscopy (SEM) data were obtained using a JEOL JSM880 microscope (15 kV, 1×10^{-8} A emission current), and all CaF_2 layers were coated with ~ 200 Å of AuPd prior to SEM characterization to reduce electron beam charging effects.

Well-defined (1×1) RHEED patterns produced by *in situ* cleaning of $\text{Si}(110)$ surfaces change dramatically as soon as growth of CaF_2 commences. Figure 1(a) shows the RHEED patterns of a CaF_2 film grown on $\text{Si}(110)$ with equivalent film thickness of < 20 Å. Long CaF_2 diffraction streaks appear along the [001] azimuth and elongated spots can be seen lying on the zeroth-order Laue zone along $[\bar{1}10]$. Fractional-order (1/3 and 2/3) spots are also clearly observable in the latter azimuth. During this initial stage, heteroepitaxy proceeds smoothly without producing 3D transmission spots.

^aElectronic mail: wliu@phyast.nhn.uokinor.edu

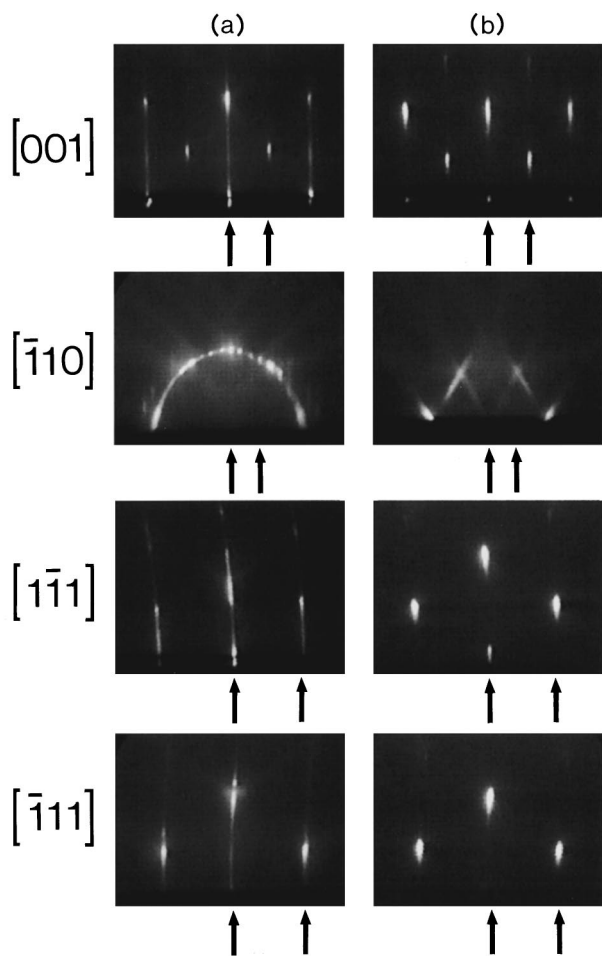


FIG. 1. RHEED patterns along the main azimuths recorded: (a) after growth of ~ 20 Å of CaF_2 and (b) after growth of ~ 200 Å of CaF_2 (arrows indicate positions of integral-order streaks).

Considerable surface ordering is present as evidenced by the (1×3) surface reconstruction observed. While the diffraction streaks in these azimuths are normal to the shadow edge, those observed in the two $\langle 111 \rangle$ azimuths are curved towards opposite directions [Fig. 1(a)]. Curved streaks in a RHEED pattern are known to result from the intersection of the Ewald sphere with two-dimensional (2D) reciprocal lattice planes arising from one-dimensional (1D) features on the real surface.¹⁰ This suggests the presence of domain structures on the surface separated by 1D domain boundaries.

At higher coverage (~ 100 Å), individual spots along $[110]$ are merged into a single ring and can no longer be resolved. This ring is not an indication of random crystal orientation since such a case will give rise to multiple concentric diffraction rings of much weaker intensities. Instead, it is indicative of one-degree orientation in which the growing surface structure has one axis preferentially aligned parallel to the incident $[110]$ electron beam.¹¹ The corresponding SEM micrograph is shown in Fig. 2(a), where the darker region was identified by energy dispersive x-ray analysis to be bare Si and the lighter region CaF_2 . The equivalent layer thickness is ~ 100 Å. Long strips of CaF_2 are seen extending along the $[110]$ direction with some irregularity at the edges [inset of Fig. 2(a)], confirming the presence of one-degree

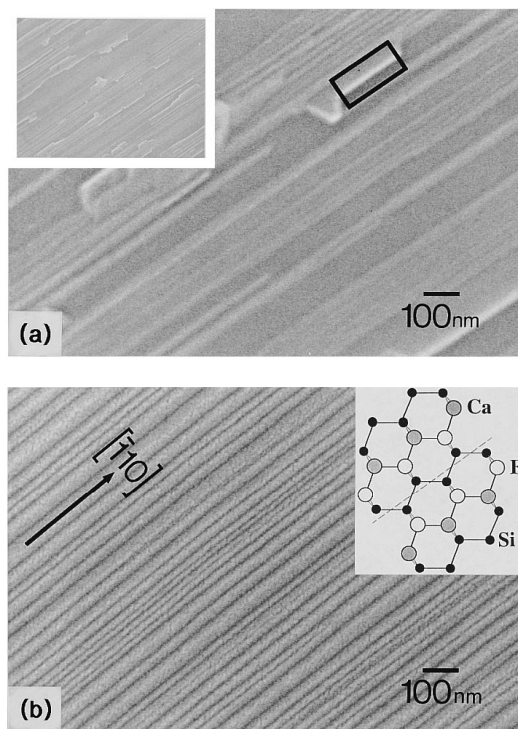


FIG. 2. SEM micrographs of the surface morphology of $\text{CaF}_2/\text{Si}(110)$ ($T_{\text{sub}} \sim 840$ °C) at different stages of growth: (a) average thickness ~ 100 Å (inset: $10 \times$ lower magnification) and (b) average thickness ~ 400 Å. The irregular ridge spacing ranges from ~ 400 – 800 Å. (Inset: plan view of a possible bonding arrangement at the $\text{CaF}_2/\text{Si}(110)$ interface relative to the ridges in the main figure).

orientation and growth anisotropy on the surface. Facet planes at the side of the ridges can also be seen in the SEM micrograph [boxed in Fig. 2(a)].

After the growth of ~ 200 Å of CaF_2 , the diffraction streaks along $[001]$ and the two $\langle 111 \rangle$ azimuths become spotty as shown in Fig. 1(b). In addition, the diffraction ring observed along $[110]$ is replaced by slanted streaks with an inscribed angle of $\sim 70^\circ$ [Fig. 1(b)]. These RHEED patterns, which remain unchanged with further growth, indicate the presence of $\{111\}$ facets on the surface. This is supported by SEM characterization of a ~ 4000 Å thick CaF_2 layer grown on $\text{Si}(110)$ at ~ 840 °C [Fig. 2(b)]. The CaF_2 surface morphology consists of long, parallel ridges with extremely straight edges and smooth sides. The ridges run along the $[110]$ direction and the sidewalls are exposed $\{111\}$ -faceted faces, which are the lowest energy surfaces for CaF_2 .¹² Other growth conditions show variations of this unusual growth morphology. For $T_{\text{sub}} < 800$ °C, the surface is dominated by misoriented grains and growth becomes increasingly $\{111\}$ oriented. This is consistent with the earlier report⁷ that the surface morphology and RHEED patterns of thick CaF_2 layers grown at $T_{\text{sub}} = 600$ °C are indistinguishable from those of layers grown on $\text{Si}(111)$ substrates. Epitaxial orientation with the $\text{Si}(110)$ substrate improves considerably with increasing substrate temperature. In particular, misoriented grains are virtually eliminated at $T_{\text{sub}} > 840$ °C. However, the CaF_2 layer, with a thermal expansion coefficient of 19.2×10^{-6} per degree compared to 2.5×10^{-6} per degree for the silicon substrate, will experience more in-plane tensile strain

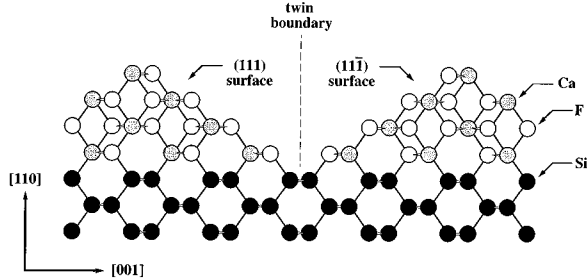


FIG. 3. Schematic illustration of the $\text{CaF}_2/\text{Si}(110)$ interface locking in the $[\bar{1}10]$ direction. Twin boundaries can originate from parallel rows of adjacent F-Si bonds. Low surface energy of the CaF_2 $\{111\}$ planes and high twin boundary interface energy result in a ridged and grooved surface morphology.

(approaching 1%) when cooled from such high growth temperatures to room temperature.

The growth anisotropy observed at the initial stage of growth can be attributed to the asymmetric bonding arrangement on the (110) growth plane. Nucleation is much more energetically and stochastically favorable along the $[\bar{1}10]$ direction where both Ca-Si and F-Si bonds can form simultaneously at the $\text{CaF}_2/\text{Si}(110)$ interface upon attachment of a single CaF_2 molecule [see inset of Fig. 2(b)], whereas two or more CaF_2 molecules are required for nucleation in the orthogonal $[001]$ direction. Such bonding also allows formation of twin boundaries since there is no restriction on the order of bonding in the (110) plane along $[001]$. It is thus possible, for example, to obtain two parallel rows of adjacent F-Si or Ca-Si bonds along the $[\bar{1}10]$ direction. Figure 3 is a schematic representation of the CaF_2/Si interface along the (110) plane which shows two twinned CaF_2 crystals with exposed low-energy $\{111\}$ faces that intersect at adjacent F-Si bonds. Continued growth of CaF_2 from this defective CaF_2/Si interface in the $[\bar{1}10]$ growth direction can result in a CaF_2 twin boundary along the (001) plane. We therefore believe that each $\{111\}$ -faceted ridge of CaF_2 on $\text{Si}(110)$ is twinned with respect to adjacent ridges and that growth is inhibited at the twin boundaries because of their high interface energy. The presence of these domain boundaries is supported by the observation of curved RHEED streaks at the very earliest stage of growth. Such twin boundaries are analogous to antiphase domain boundaries in GaAs grown on Si and may be reduced by growth on off-axis (110) substrates.

A ridged and grooved surface morphology is not incompatible with solid state microlaser fabrication. In fact, the $\{111\}$ -faceted ridges can function as two sides of a triangular-shaped waveguide for confinement of light along the $[\bar{1}10]$ direction. Therefore, even though CaF_2 grown on $\text{Si}(110)$ has a nonplanar surface morphology, such layers can still be promising candidates for fabrication of rare-earth-doped CaF_2 lasers on Si. A ridged CaF_2 surface morphology may actually help reduce multimode emission from laser struc-

tures fabricated from this material. Our own preliminary rare-earth doping experiments¹³ show that there is no significant difference among photoluminescence emission intensities from CaF_2 layers grown on (110), (100), or (111)-oriented substrates. We therefore conclude that it is possible to fabricate rare-earth doped CaF_2 microlasers on $\text{Si}(110)$ substrates. However, since the refractive index of CaF_2 ($n=1.43$) is smaller than that of Si ($n=3.44$), further work has to be done in designing the waveguide structure to achieve efficient light confinement within the CaF_2 layer.

In summary, we report the use of RHEED and SEM to study the growth mode of CaF_2 on $\text{Si}(110)$. Our results show that CaF_2 growth is initiated by 1D nucleation of CaF_2 ridges parallel to the $[\bar{1}10]$ direction due to asymmetric bonding arrangement on the (110) surface. Low-energy $\{111\}$ facets develop and a ridged and grooved surface morphology results. Further growth occurs via stacking of $\{111\}$ planes on the sidewalls of the ridges. This surface morphology is believed to result from the combination of favorable energetics in exposing the low-energy $\{111\}$ facets and the presence of twinned crystallographic domains. Twin boundaries can originate from random attachment of CaF_2 molecules to the Si substrate such that parallel rows of adjacent F-Si (and/or Ca-Si) bonds occur along the $[\bar{1}10]$ direction. The optimum substrate temperature range for (110)-oriented epitaxy was found to be between 800 and 900 °C.

We thank Matthew Johnson and Mike Santos for helpful discussions, Bill Chissoe for assistance in the SEM studies, and Joel Young for technical support. This work was partially supported by the National Science Foundation through Grant No. OSR-9108771.

- ¹L. J. Schowalter and R. W. Fathauer, *Crit. Rev. Solid State Mater. Sci.* **15**, 367 (1989), and references therein.
- ²R. A. McFarlane, M. Lui, and D. Yip, *IEEE J. Selected Topics Quantum Electron.* **1**, 82 (1995).
- ³M. Lui, R. A. McFarlane, and D. Yap, *Mater. Res. Soc. Symp. Proc.* **329**, 167 (1994).
- ⁴M. Lui, R. A. McFarlane, D. Yip, and D. Lederman, *Electron. Lett.* **29**, 172 (1993).
- ⁵C. C. Cho, W. M. Duncan, T. H. Lin, and S. K. Fan, *Appl. Phys. Lett.* **61**, 1757 (1992).
- ⁶A. S. Barriere, S. Raoux, A. Garcia, H. L' Haridon, B. Lambert, and D. Moutonnet, *J. Appl. Phys.* **75**, 1133 (1994).
- ⁷L. J. Schowalter, R. W. Fathauer, L. G. Turner, and C. D. Robertson, *Mater. Res. Soc. Symp. Proc.* **37**, 151 (1985).
- ⁸A. Ishizaka and Y. Shiraki, *J. Electrochem. Soc.* **133**, 666 (1986).
- ⁹X. M. Fang, P. J. McCann, and W. K. Liu, *Thin Solid Films* (to be published).
- ¹⁰B. A. Joyce, J. H. Neave, P. J. Dobson, and P. K. Larsen, *Phys. Rev. B* **29**, 814 (1986).
- ¹¹E. Bauer, in *Techniques for the Direct Observation of Structure and Imperfections Part 2*, edited by R. F. Bunshah (Interscience, New York, 1969), pp. 501-557.
- ¹²P. W. Tasker, *J. Phys. (Paris) Colloq.* **41**, C6 (1980).
- ¹³P. J. McCann, X. M. Fang, T. Chatterjee, W. Shan, and J. J. Song, *American Association for Crystal Growth Conference*, Fallen Leaf Lake, CA, 4-7 June 1995.